Computational investigation on the catalytic activity of Rh6 and Rh4Ru2 clusters towards methanol activation

ARTICLE *in* THEORETICAL CHEMISTRY ACCOUNTS · DECEMBER 2014

Impact Factor: 2.23 · DOI: 10.1007/s00214-014-1597-z

4 AUTHORS:

Kamalika Ghatak

CSIR - National Chemical Laboratory, Pune

5 PUBLICATIONS **29** CITATIONS

SEE PROFILE

Turbasu Sengupta

CSIR - National Chemical Laboratory, Pune

4 PUBLICATIONS **0** CITATIONS

SEE PROFILE

Sailaja Krishnamurty

Central Electrochemical Research Institute

54 PUBLICATIONS **885** CITATIONS

SEE PROFILE

Sourav Pal

CSIR - National Chemical Laboratory, Pune

180 PUBLICATIONS **2,820** CITATIONS

SEE PROFILE

Computational Investigation on the Catalytic Activity of Rh_6 and Rh_4Ru_2 Clusters Towards Methanol Activation

Kamalika Ghatak, Turbasu Sengupta, Sourav Pal *

Physical Chemistry Division, CSIR–National Chemical Laboratory, Pune, India; s.pal@ncl.res.in

Sailaja Krishnamurty

Functional Materials Division, CSIR–Central Electrochemical Research Institute, Karaikudi, India; sailaja.raaj@gmail.com

Abstract

Catalysis of molecular activation of small molecules through scission of strong chemical bonds is one of the major challenges faced by chemists. More specifically, activation of the strong C–H and O–H bonds of various alcohols, especially methanol, is one of the various important intermediate steps of key organic reactions. Our present work explores a suitable metal cluster catalyst towards methanol dissociation. In particular we have examined the effect of ruthenium doping (Rh:Ru=2:1) on the catalytic activity of Rh_6 cluster towards methanol dissociation. Density functional theory based calculations illustrate two competitive pathways for methanol dissociation, which are via O–H and C–H bond breaking. Both the pathways are found to be energetically favourable in presence of bimetallic and mono-metallic clusters. Importantly, energy barrier for O–H bond dissociation reduces considerably in doped cluster as compared to pure Rh_6 cluster and is smaller than the values reported for a number of other small metallic clusters.

Keywords. Methanol Activation, Density Functional Theory (DFT), Rhodium Clusters, Doping, Bimetallic Clusters.

I. Introduction

Methyl alcohol, commonly known as methanol, is the simplest alcohol and one of the most versatile compound having multi-fold applications in areas such as, (a) organic synthesis, (b) transportation fuel, (c) waste water denitrification, d) production of pure hydrogen, also known as steam reforming, and most importantly e) in fuel cells. Methanol is a liquid between -97.0 ºC to 64.7 ºC at atmospheric pressure and hence is an ideal fuel for transportation in large parts. Since it is produced from natural gases, it is cost effective and non renewable in nature. Methanol (MeOH) has higher hydrogen content as compared to H_2 stored in cylinders or hydrides leading to lower system weight and volume. A necessary step in almost all applications regarding methanol requires the activation of its O–H and C–H bonds. Activation of strong organic bonds is one of the major challenges in chemistry due to its indispensability towards developing more and more cost-effective paths in industrial production of chemicals. Among them, controlled scission of strong O-H and C-H bonds of aliphatic alcohol, especially methanol, is one of the important steps. This is a fairly difficult process given the high energy required to dissociate the C–H (~96.1 kcal/mol) and O–H (~104.6 kcal/mol) bonds. In this respect, few of the earlier works have attempted to evaluate activation barrier for the first step of the methanol dissociation from different pathways.

In this context, many theoretical studies have focussed in identifying metal oxide and metal surfaces with moderate to low barrier towards either O–H or C–H activation. TiO_2 is the most well studied metal oxide for methanol activation. In a recent theoretical work by Sanchez et al., the dissociation of O–H on TiO_2(101) (anatase) surface is investigated, and the activation barrier for O–H bond scission is reported to be as low as 13.6 kcal/mol. Methanol decomposition on noble metal surfaces has gained importance from the point of view of heterogeneous catalysis. In spite of many successes in this field, the exact effect of surface defects and structural dependence on catalysis has not been fully understood yet. A work based on methanol activation on Pt(111) surface reports substantially high barriers for both the O–H (~22 kcal/mol) and C–H (~34 kcal/mol) bond scissions, whereas slightly lower barriers of 12.7 kcal/mol (C–H scission) and 24.7 kcal/mol (O–H scission) are reported for Pd(111) surface. In a very recent work, stepped Pd(211) surface is shown to lower the O–H activation barrier (18.9 kcal/mol) but C–H activation barrier (14.7 kcal/mol) is seen to be slightly higher than in case of Pd(111) surface. Cu surfaces

are also one of the well studied metal surfaces in activating methanol. The barriers for O-H dissociation on a Cu(100) surface is 14.5 kcal/mol while elevated barrier(24.6 kcal/mol) were reported on a Cu(111) surface. Recently, Wang et al. reported competitive barriers for C–H (12 kcal/mol) and O–H (12.4 kcal/mol) activation on Ir(111) surface with slightly endothermic reaction energies.

Small metal clusters form another class of materials being actively explored as candidates towards methanol activation. Methanol activation studies on Cu_4, Co_4 and Pd_4 atomic clusters reveal that Co_4 cluster is catalytically more active having lower energy barrier towards both O–H scission (10.8 kcal/mol) and C–H scission (14.3 kcal/mol). In another work by Xie et al., combined theoretical and experimental investigation reveals O–H activation to be more favorable over C–H activation on neutral iron clusters. Al_n clusters are seen to have size selective reactivity towards methanol molecule and its O–H bond dissociation. V_3^+ cluster is reported to possess a moderate barrier of 13.9 kcal/mol towards O–H activation. In addition, several other metal clusters such as: Au_n, Ni_n^+, Pt-Au, and $Cu_nAu_m^+$ have been explored for their potential towards methanol activation.

Rhodium clusters have been a subject of numerical experimental and theoretical studies due to their catalytic properties. Rh clusters are now well established catalysts for applications such as, a) controlling automobile exhaust emissions (CO, NO, NO_2 etc.), b) reforming fuels such as biogas and diesel, c) oxidation reduction reactions, d) reverse hydrogen spill over reaction, e) hydrogenation of alkenes, f) conversion of syngas etc. High activity and thermal stability make Rh based nanoclusters very attractive particularly in fuel cell electro-catalysts and hence, attempts are being made to synthesize extremely small Rh clusters. Among various rhodium clusters, Rh_6 is an efficient cluster due to its high catalytic activity in several reactions. Earlier theoretical studies suggest an octahedral ground state geometry for the same. Doping these Rh clusters further improves and enhances the catalytic activity and also reduces the disadvantages that are present in homogeneous Rh catalysts.

Rh-Pt binary clusters are the most popular catalysts towards alcohol oxidation in Direct Alcohol Fuel Cells (DAFC). While Rh is known to inhibit the CO poisoning, Ru is well known to increase the rate of methanol oxidation reactions when doped with platinum. Hence, we explore the unique combination of Rh–Ru binary clusters to have best of both sides. Hence, we explore the potential catalytic activity of pure Rh clusters and Ru doped Rh clusters for methanol oxidation. In this present article, we study the properties of an octahedral Rh_6 cluster towards methanol activation. In order to explore the potential of Ru doping towards methanol activation, we have replaced

two of the trans rhodium atoms by ruthenium atoms leading to a Rh_4Ru_2 (Rh:Ru = 2:1) cluster. It is of relevance here to note that bimetallic clusters having 2:1 ratio can be commonly synthesized experimentally and hence we have used this ratio in our present study. The principal objective of the study is to understand the detailed interaction of methanol molecule with these clusters and their effectiveness towards activation of C–H and O–H bonds in methanol molecule.

II. Computational Details

We have considered the lowest spin state for all the clusters in our study. Around ten Rh_6 conformations are considered in the lowest spin state to begin with. Optimization of these conformations revealed the octahedral geometry to be the most stable one among all the conformations. Some of the earlier reported studies also considered Rh_6 cluster in its lowest spin state. All the calculations in this work are performed using Density Functional Theory (DFT) as implemented in Gaussian 09 package. The geometries are optimized using PBE-PBE functional with LANL2DZ basis set along with LANL2 effective core potential (pseudo potential) for the core electrons of metal atoms. TZVP basis set is used for the rest of the atoms. PBE-PBE is widely used for transition and as well as other metal clusters and complexes. Following geometry optimization, harmonic frequencies are calculated for all the optimized conformations. All the frequencies are found to be positive, indicating the conformations to be local minimum. The transition state conformations have one imaginary frequency (with high magnitude), signifying the first order saddle point. The transition state barriers are calculated from the corresponding free energies. As implemented in Gaussian 09 package, the absolute value of total free energy (G_{tot}) considered for each structure is calculated using the Gibbs free energy function in terms of enthalpy (H_{tot}) and entropy (S_{tot}) :

$$G_{tot} = H_{tot} - TS_{tot} = E_{tot} + PV - TS_{tot}$$

where E_{tot} is represented by its individual components like electronic, translational, rotational, vibrational and contribution from zero point energy correction. Hence,

$$G_{tot} = E_{elec} + E_{trans} + E_{rot} + E_{vib} + E_{ZPE} + PV - TS_{tot} = E_{elec} + G_{therm}$$

where G_{therm} is the thermal free energy.

Contribution of each component to total internal energy (E_{tot}) is calculated using the derived partition function for that particular component using the following formula:

$$E = Nk_bT^2\left(\frac{\partial \ln Z}{\partial T}\right)_V$$

where Z is the partition function of the corresponding component and k_b is the Boltzmann constant. For 1 mol of gas, N is replaced by Avogadro's number (N_A) and hence the equation reduces to

$$E = RT^2\left(\frac{\partial \ln Z}{\partial T}\right)_V$$

Similarly the total entropy S_{tot} can be written in terms of its component by the following formula:

$$S_{tot} = S_{trans} + S_{rot} + S_{vib} + S_{elec}$$

The entropic contribution per mol for each component is derived from the following equation:

$$S = RT\left(\frac{\partial \ln Z}{\partial T}\right)_V + R\ln Z$$

Zero point energy (*ZPE*) correction for each vibrational mode is also incorporated within our calculations. Total *ZPE* correction including *3N-6* modes of vibration (*3N-5* for linear molecule) is represented as follows:

$$E_{ZPE} = \sum_{i=1}^{3N-6} \tfrac{1}{2} h\upsilon_i$$

where ν_i is the frequency of the corresponding mode of vibration.

Binding Energy (BE) of the clusters is calculated using:

$$\frac{BE}{atom} = \frac{E_{cluster} - \sum_{i=1}^{N} E_i}{N}$$

where, N is the number of metal atoms in the cluster, E_i is the free energy of an atom and $E_{cluster}$ is the free energy of the total cluster. Charge analysis of the systems is based on the Mulliken partitioning scheme.

Following the structural and electronic property analysis of Rh_6 and Rh_4Ru_2 clusters, their thermal stability is examined by carrying out Born Oppenheimer Molecular Dynamics (BOMD) simulations using the deMon2K package. The finite temperature simulations are carried out on Rh_6 and Rh_4Ru_2 clusters from 300 K to 700 K with a temperature interval of 100 K. Thermal stability and finite temperature behaviour of the methanol adsorbed Rh_6 and Rh_4Ru_2 clusters is verified by performing a simulation at 300 K on the complexes. For each simulation, the cluster is equilibrated for a time period of 10 ps followed by a simulation time of 40 ps. The temperature of the cluster is

maintained using Berendsen's thermostat (τ = 0.5 ps) in an NVT ensemble. The nuclear positions are updated using the velocity verlet algorithm with a time step of 1 fs. We hold the total angular momentum of the cluster to zero thereby suppressing the cluster rotation.

III. Results and Discussions

We begin with a discussion on the geometry of optimized structure of Rh_6 cluster as shown in Fig. 1. The structure has Rh–Rh bond distances of 2.55 Å for the adjacent atoms. The calculated binding energy/atom of this Rh_6 cluster is -2.76 eV/atom. The bond distances and binding energy of this cluster are in agreement with previously reported values for Rh_6 cluster using different functional. In order to have a Rh–Ru bimetallic cluster in 2:1 ratio having a heterogeneous environment, two diagonally opposite Rh atoms in octahedral Rh_6 are replaced by Ru atoms as shown in Fig. 1. This type of heterogeneous environment has already been shown to be important for effective activation and dissociation of C–H and O–H bonds in methanol. The fully optimized geometry of Rh_4Ru_2 cluster (see Fig. 1) is found to retain the octahedral conformation with a little distortion in the inter-atomic bond lengths with respect to its parent Rh_6 cluster. The Rh–Rh bond distances increase to 2.58 Å and bonded Rh–Ru bond distances are found to lie between 2.52 to 2.53 Å. Our calculated binding energy/atom for bimetallic cluster is -2.90 eV/atom, which is significantly greater as compared to its mono-metallic counterpart. A comparative Mulliken charge analysis reveals that all the atoms in Rh_6 are neutral. On doping, Rh atoms in Rh_4Ru_2 gain approximately 0.03 electrons each from Ru atoms (see Table. 1 of the supporting information). This small amount of charge separation in Rh_4Ru_2 is suggestive of its higher potential towards methanol activation as compared to Rh_6. Most of the monometallic or bimetallic clusters, in spite of their excellent catalytic properties, do not have practical applications due to their thermodynamic instability. Hence, before analyzing the catalytic property of bimetallic clusters, we have studied the thermodynamic behaviour of both the clusters by performing finite temperature BOMD simulations from 200 K to 700 K with an interval of 100 K. The simulations revealed that both the clusters retain their octahedral conformations up to at least 700 K.

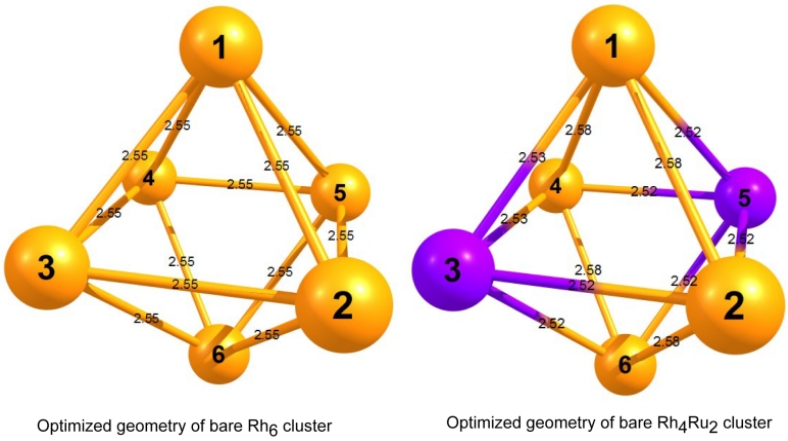

Fig. 1 Structural parameters in Rh_6, Rh_4Ru_2 clusters (golden coloured atom: Rh; purple coloured atom: Ru)

A. Structural and Electronic Properties of Methanol Adsorbed Rh_6 and Rh_4Ru_2 Clusters:

All sites are chemically equivalent in the Rh_6 cluster. On the other hand, it is difficult to predict the center (either Rh or Ru) that is more favourable for adsorption of methanol molecule in Rh_4Ru_2 cluster. Though the charge analysis of Rh_4Ru_2 indicates that Ru center is a more favourable site (as it has small amount of positive charge) for methanol adsorption through oxygen atom, the following two orientations have been optimized, viz., a) orientation-I where methanol is adsorbed on the Ru center through the oxygen atom and b) orientation-II where methanol is adsorbed on the Rh center through the oxygen atom. Orientation-I is found to be energetically more stable by 5.7 kcal/mol with respect to the orientation-II (see Fig. 2). Differences in thermodynamic stabilities can be attributed to the greater charge separation between Ru and O atoms in orientation-I, leading to greater electrostatic interactions as compared to those in orientation-II (see Table. 2 of the supporting information).

Upon adsorption of methanol (MeOH) on Rh_6 and Rh_4Ru_2 clusters (orientation-I as well as orientation-II) (Fig. 3), C–O bond length elongates by 0.2 Å (the C–O bond length is 1.43 Å in free methanol molecule). The C–H and O–H bond lengths in the adsorbed methanol are found to be similar as in free methanol. However, differences in bond lengths are observed for the M–O (M = Rh/Ru) bonds ($Ru–O_{orient\text{-}I}$ bond length= 2.27 Å; $Rh–O_{orient\text{-}II}$ bond length=2.29 Å; Rh–O bond length = 2.33 Å). Thus, Metal-Oxygen bond distance is slightly elongated in monometallic cluster as compared to the bimetallic Rh_4Ru_2 clusters. Interestingly, significant elongation in two of

the Rh–Rh bond lengths (2.96 Å) is observed in case of the Rh_4Ru_2-$MeOH_{orient\text{-}II}$, leading to a slightly distorted octahedral structure (see Fig. 3c).

It is pertinent to take a close look at the thermodynamics of these methanol–adsorbed complexes and hence free energy of formation ($G_{formation}$) is calculated. Corresponding thermodynamic stability is evaluated by the following method:

$$G_{formation} = G_{complex} - \left(G_{cluster} + G_{MeOH} \right)$$

where, $G_{complex}$, $G_{cluster}$ and G_{MeOH} are the absolute free energies for the cluster–MeOH complex, cluster and a single methanol molecule respectively. $G_{formation}$ (free energy of formation) of the Rh_6–(MeOH) complex is found to be -0.62 kcal/mol, while $G'_{formation\text{-}orient\text{-}I}$ and $G'_{formation\text{-}orient\text{-}II}$ (free energy of formation of the Rh_4Ru_2–(MeOH) complex of orient-I and orient-II respectively) are found to be -17.9 kcal/mol and -12.2 kcal/mol thereby suggesting greater thermodynamic stability of bimetallic-MeOH complexes as compared to the Rh_6–MeOH complex. It is very important to mention here that adsorption of methanol results in significant charge separations in both orientations of the Rh_4Ru_2–(MeOH) complex as compared to the charge separation in Rh_6–(MeOH) complex (see Table. 2 of the Supporting Information).

The difference in the values of $G_{formation}$ and $G'_{formation}$ can be further correlated following the analysis of frontier orbitals of both the complexes. HOMO of both Rh_4Ru_2–(MeOH) complexes show bonding character whereas the Rh_6–(MeOH) complex has non-bonding interactions (see Fig. 4). BOMD simulations at 300 K on both the Rh_4Ru_2–(MeOH) complexes demonstrate that the complexes do not undergo significant structural transformations and the molecule remains adsorbed on the cluster at this temperature. BOMD simulation at 300 K on Rh_6–(MeOH) complex also reveals the complex to be stable with methanol molecule undergoing rapid movements. This is easily demonstrated in the variations of Rh–O bond length as a function of time in Rh_6–(MeOH) complex (see Fig. 1 of the supporting information). On the other hand, Ru–O bond length in orientation-I and Rh–O bond length in orientation-II of Rh_4Ru_2–(MeOH) complexes equilibrate towards the end of the simulation (see Fig. 2 and 3 of the Supporting Information). All the above mentioned facts contribute together to the higher values of $G'_{formation}$. Finally, all the methanol adsorbed complexes show negative free energy of formation and are thus thermally stable. Next, we evaluate the efficiency of individual complexes towards methanol dissociation kinetics in the following section.

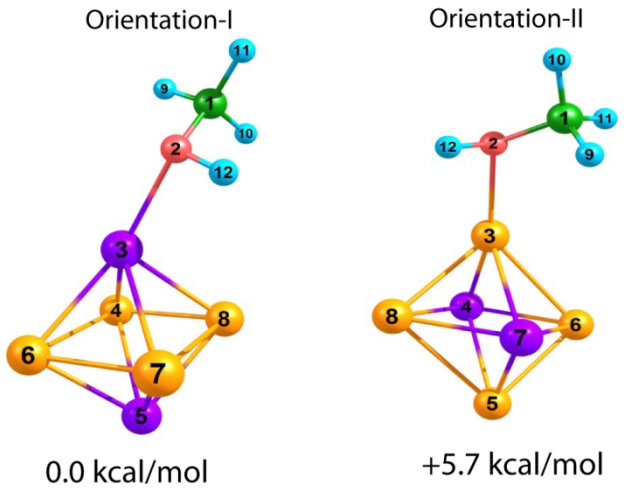

Fig. 2 Relative energies of Rh_4Ru_2–$(MeOH)_{orient\text{-}I}$ and Rh_4Ru_2–$(MeOH)_{orient\text{-}II}$ complexes

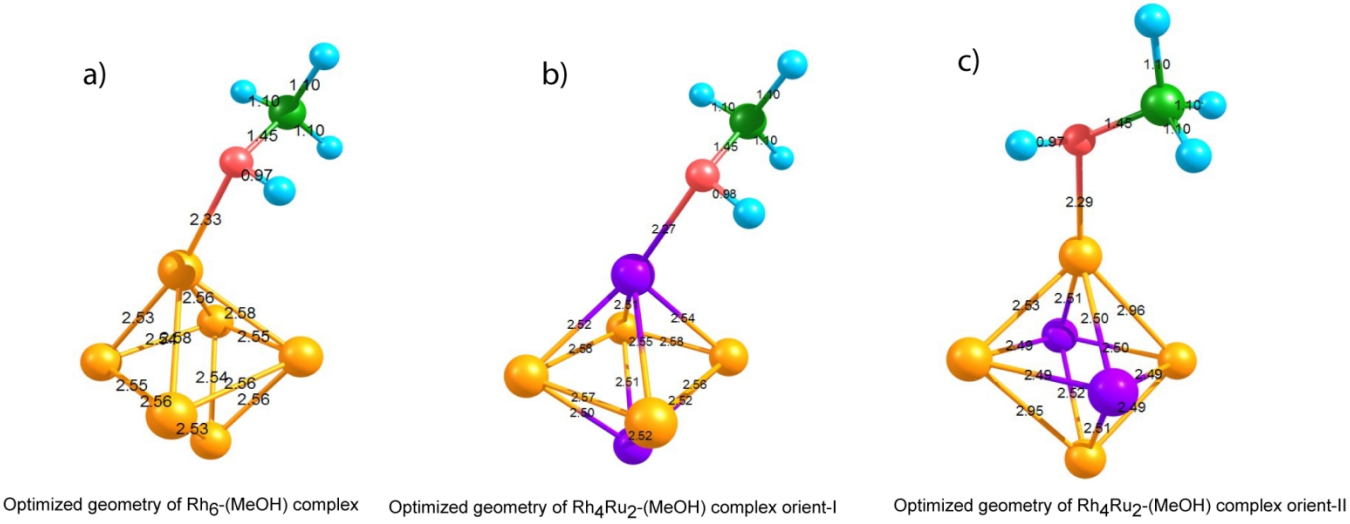

Fig. 3 Optimized geometry for methanol adsorbed (a) Rh_6, (b) Rh_4Ru_2 in orientation-I and (c) Rh_4Ru_2 in orientation-II clusters. (golden: Rhodium; purple : Ruthenium; green: Carbon; red: Oxygen; sky blue : Hydrogen)

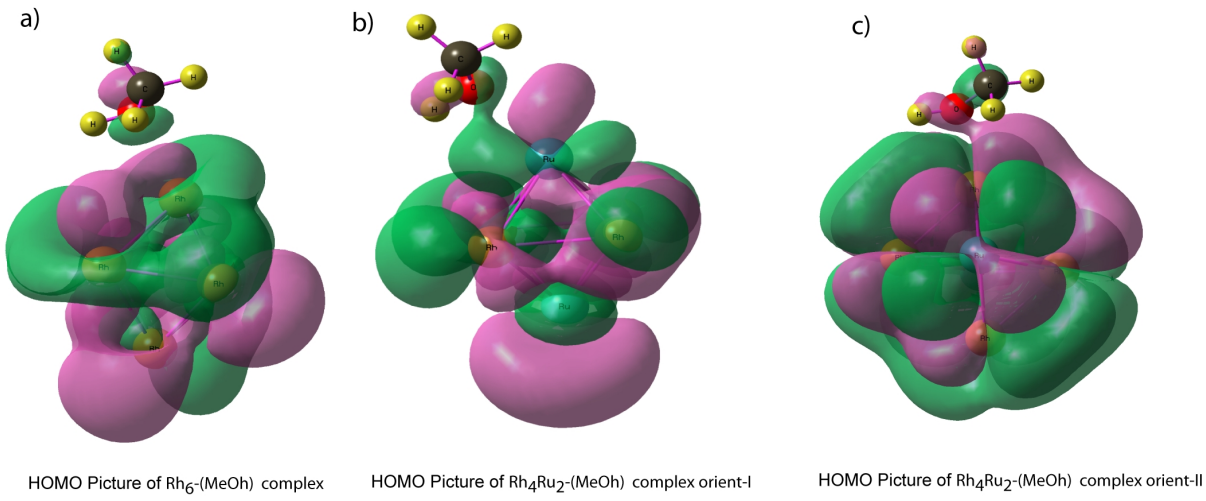

Fig. 4 HOMO of methanol adsorbed (a) Rh_6, (b) Rh_4Ru_2 in orientation-I and (c) Rh_4Ru_2 in orientation-II Clusters.

B. Methanol Dissociation on Rh_6 and Rh_4Ru_2 Clusters

Our present study focuses on the catalytic activities of these clusters towards the dissociation of C–H and O–H bonds of single methanol molecule. Corresponding barriers for both the clusters are calculated and are used as indicators of catalytic activity throughout the remaining article.

1. Dissociation of O–H bond in methanol: Transition state corresponding to the O–H bond dissociation of methanol in presence of Rh_6 catalyst involves the breaking of the O–H bond and transfer of hydrogen atom to any one of the consecutive Rh atoms. The barrier for the same is obtained to be 13.9 kcal/mol (ΔG) (see Fig. 5a). The transition states corresponding to O-H bond dissociation in Rh_4Ru_2 clusters are shown in Fig. 5b and Fig. 5c. It is clear that both the orientations require less energy to dissociate the O–H bond in methanol. The reason behind lower O-H dissociation barrier in Rh_4Ru_2 is due to the fact that this reaction requires smaller stretching of the O–H bond as compared to that in Rh_6 species. The bond between the oxygen and hydrogen atoms (corresponding to the transition state geometry) is stretched to a greater extent in case of Rh_6 as compared to the bimetallic cases. The O–H distance is 1.57 Å in the transition state corresponding to the Rh_6 cluster as compared to 1.35 Å and 1.48 Å in the transition states involving Rh_4Ru_2 cluster in orientation-I and orientation-II, respectively (O–H bond distance in free methanol molecule is 0.99 Å). Incorporation of a second metal atom in the Rh_6 cluster significantly increases the charge

separation between the atoms in the bare cluster (Table. 1 of the supporting information) and as well as in complexes (see Table. 2 of the supporting information), leading to a more reactive cluster. HOMOs corresponding to the transition states of Rh_4Ru_2 cluster in both orientations (Fig. 4 of the supporting information) also account for the lower O–H dissociation barrier. In the bimetallic cases, the "*s*" orbital of the concerned hydrogen overlaps with the "*d*" orbital of the metal atom and thus provides some degree of stabilization to this particular transition state. Such an overlap is absent in the case of Rh_6 cluster. Finally, for the sake of completeness, we also calculated the activation barrier for methanol on Ru_6 cluster (a prism conformation which has the lowest energy among other conformations) which was found to be 17.5 kcal/mol (see Fig. 6a of the Supporting Information). Thus, Rh–Ru bimetallic clusters lower the activation barrier for methanol as compared to both the mono-metallic parent clusters.

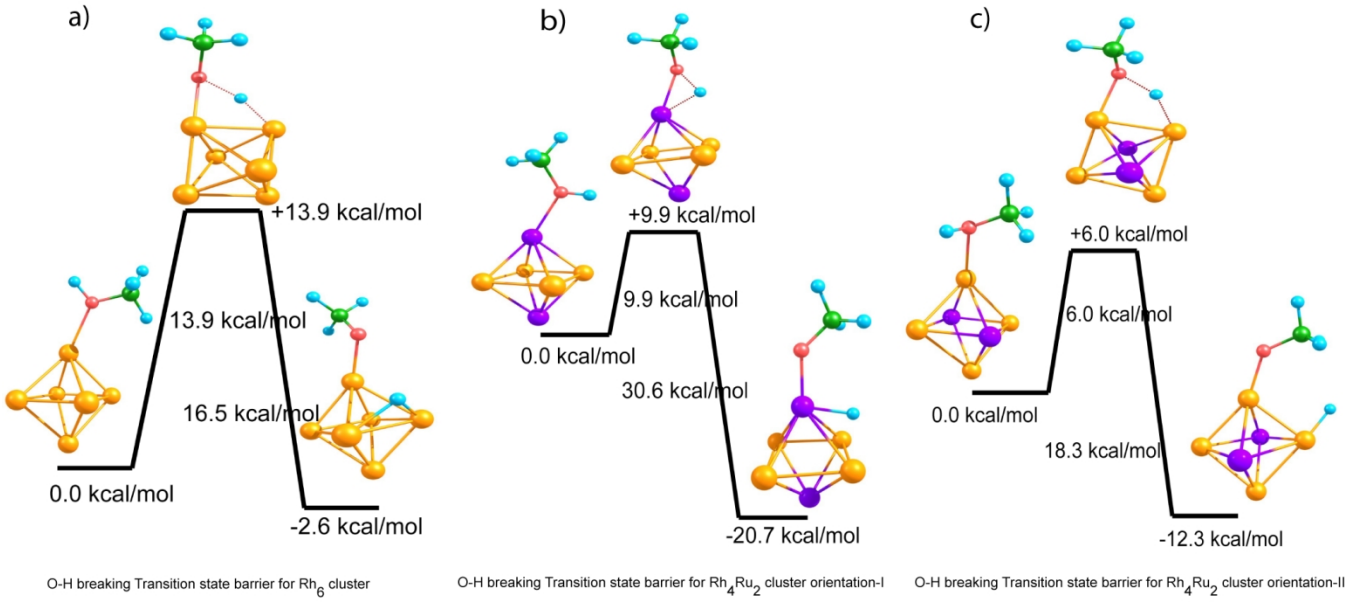

Fig. 5 Transition barrier for O–H bond dissociation in methanol adsorbed (a) Rh_6, (b) Rh_4Ru_2 in orientation-I and (c) Rh_4Ru_2 in orientation-II clusters. (golden: Rhodium; purple: Ruthenium; green: Carbon; red: Oxygen; sky blue : Hydrogen)

2. Dissociation of C–H bond in methanol: Transition states corresponding to the C–H bond dissociation are calculated for both the orientations of the bimetallic cluster and the Rh_6 cluster. The activation barrier for methanol on Ru_6 cluster is found to be 13.4 kcal/mol (see Fig. 6b of the supporting information) Transition state corresponding to the Rh_6 cluster has moderate barrier height of 13.6 kcal/mol (shown in Fig. 6a). However, reduction in the barrier

heights (by 1.7 kcal/mol and by 2.7 kcal/mol for orientations I and II, respectively) is observed in case Rh_4Ru_2 cluster (Fig. 6b and 6c). Furthermore, the product corresponding to the Rh_6 cluster is found to be endothermic (+3.5 kcal/mol) with respect to the reactant, whereas the products corresponding to the Rh_4Ru_2 clusters are exothermic in nature. The difference in energy between these pathways can also be explained from the point of view of C–H bond stretch in the corresponding transition state structures which is found to be 1.53 Å in Rh_6 as compared to 1.44 Å in orientation-I and 1.48 Å in orientation-II of Rh_4Ru_2 clusters.

Unlike the O–H dissociation process, it is clear from the frontier orbital pictures (see Fig. 5a and 5b of the supporting information) of this particular transition state that the dissociated hydrogen atom lacks proper stabilizing interaction with the adjacent Rh atom in Rh_6 cluster and orientation-I of Rh_4Ru_2 cluster. On the other hand, in case of orientation-II, the dissociated hydrogen gets slight stabilization due to the overlap of the corresponding metal and hydrogen orbitals (Fig. 5c of the supporting information). It is to be noted here that HOMO picture of transition state structure involving Rh_6 cluster suggests more of an anti-bonding character, whereas non-bonding(orientation-I)/bonding(orientation-II) interactions are observed for Rh_4Ru_2 cases, which accounts for the slightly elevated barrier height in case of Rh_6 as compared to Rh_4Ru_2.

As orientation-I is the lowest energy conformation of the Rh_4Ru_2–(MeOH) complex (Fig. 2), the total barrier height of the corresponding O–H and C–H activation for orientation-II (Fig. 5c and 6c) are 11.7 kcal/mol and 16.6 kcal/mol (ΔG) respectively, following the addition of the stabilisation energy of 5.7 kcal/mol (Fig. 2) to the calculated barrier heights (Fig. 4 c and 5 c). Therefore, from Fig. 5 and 6 it is clear that the transition states corresponding to both O–H and C–H activation will be more favourable for the orientation-I of the Rh_4Ru_2–(MeOH) complex.

In short, in our calculations we have considered two competitive pathways (O–H breaking and C–H breaking) for the commencement of methanol dissociation in presence of rhodium and rhodium-ruthenium clusters. Our investigation reveals that the initiation of methanol dissociation is kinetically more favoured to occur via the O–H breaking pathway in presence of both the clusters. The solution regarding the choice of a better catalyst can be inferred from both thermodynamic and kinetic point of view. The overall activation barrier for O–H dissociation is lower for orientation-I of Rh_4Ru_2 cluster as compared to the Rh_6 cluster. Since the energy difference between both the orientations of methanol adsorbed Rh_4Ru_2 complexes is not very high, formation of a small amount Rh_4Ru_2–

$(MeOH)_{orient\text{-}II}$ is highly probable along with the Rh_4Ru_2–$(MeOH)_{orient\text{-}I}$, resulting in even lower O–H activation barrier (6.0 kcal/mol ; see Fig. 5c). Negative $G_{reaction}$ values (shown in Fig. 5) for all the cases also indicate that all the reactions are exothermic in nature, however the products are found to be more stable ($G_{reaction}$= -20.7 kcal/mol and -12.3 kcal/mol for orient-I and orient-II respectively) in both the Rh_4Ru_2 cases. Our computational investigation thus reveals that both the clusters favour the O–H dissociation path but Rh_4Ru_2 cluster is catalytically more active towards initiation of methanol dissociation.

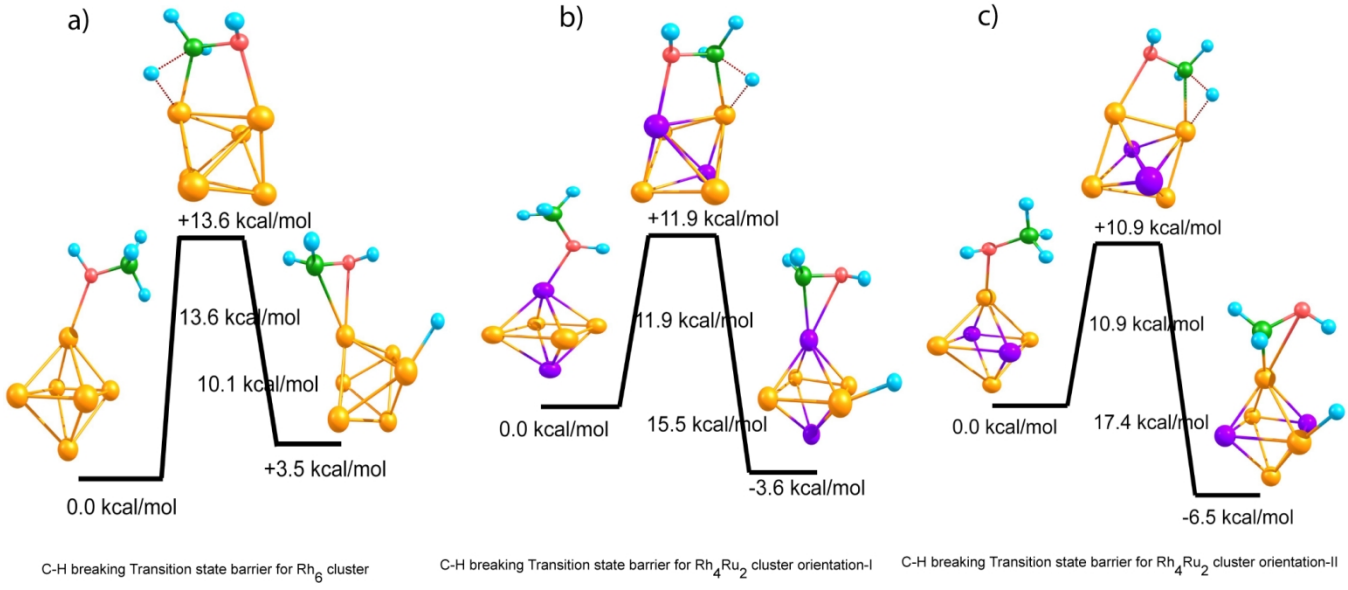

Fig. 6 Transition barrier for C–H Bond dissociation in methanol adsorbed (a) Rh_6, (b) Rh_4Ru_2 in orientation-I and (c) Rh_4Ru_2 in orientation-II clusters. (golden: Rhodium; purple: Ruthenium; green: Carbon; red: Oxygen; sky blue : Hydrogen)

IV. Conclusions

The present article investigates the potential of bimetallic Rh_4Ru_2 and pure Rh_6 clusters towards methanol activation and explores that both the clusters are well suited towards the same using DFT methodology. It has been shown that ruthenium doping enhances the reactivity of the parent cluster by creating a heterogeneous environment. In other words, Rh_4Ru_2 is found to possess higher catalytic activity towards the initiation of methanol dehydrogenation. Our study indicates that dehydrogenation of methanol occurs through the O–H bond scission. It is important to note here that our calculated bond dissociation barriers are lower than some previously reported metal clusters (Co_4, Pd_4, Cu_3

etc.) and catalytic surfaces (Cu(111), Pd(111), Ir(111) etc.) as well. Thus, catalytic activity of this bimetallic catalyst can be further explored towards activation of other small molecules such as CO, HCOOH, NH_3BH_3 etc. and such studies are presently under consideration.

Acknowledgements

The authors acknowledge the Center of excellence in Computational Chemistry at CSIR–NCL, Pune, for the calculations presented and the CSIR XIIth 5–year plan for a Multiscale Simulation of Materials (MSM) project grant. Sourav Pal acknowledges grant from SSB project of CSIR and the J. C. Bose Fellowship grant of DST towards partial fulfillment of this work. Kamalika Ghatak acknowledges Mr. Susanta Das and Mr. Dar Manzoor of CSIR-NCL for special discussions.

References

1. Blank B, Michlik S, Kempe R (2009) Synthesis of Selectively Mono-N-Arylated Aliphatic Diamines via Iridium-Catalyzed Amine Alkylation. Advanced Synthesis & Catalysis 351 (17):2903-2911. doi:10.1002/adsc.200900548

2. Grigg R, Mitchell TRB, Sutthivaiyakit S, Tongpenyai N (1981) Oxidation of alcohols by transition metal complexes part V. Selective catalytic monoalkylation of arylacetonitriles by alcohols. Tetrahedron Letters 22 (41):4107-4110. doi:http://dx.doi.org/10.1016/S0040-4039(01)82078-5

3. Moran J, Preetz A, Mesch RA, Krische MJ (2011) Iridium-catalysed direct C–C coupling of methanol and allenes. Nat Chem 3 (4):287-290. doi:http://www.nature.com/nchem/journal/v3/n4/abs/nchem.1001.html#supplementary-information

4. Vancoillie J, Demuynck J, Sileghem L, Van De Ginste M, Verhelst S (2012) Comparison of the renewable transportation fuels, hydrogen and methanol formed from hydrogen, with gasoline – Engine efficiency study. International Journal of Hydrogen Energy 37 (12):9914-9924. doi:http://dx.doi.org/10.1016/j.ijhydene.2012.03.145

5. Pan Y, Ye L, Ni B-J, Yuan Z (2012) Effect of pH on N2O reduction and accumulation during

denitrification by methanol utilizing denitrifiers. Water Research 46 (15):4832-4840. doi:http://dx.doi.org/10.1016/j.watres.2012.06.003

6. Pan Y, Ni B-J, Bond PL, Ye L, Yuan Z (2013) Electron competition among nitrogen oxides reduction during methanol-utilizing denitrification in wastewater treatment. Water Research 47 (10):3273-3281. doi:http://dx.doi.org/10.1016/j.watres.2013.02.054

7. Timmermans P, Van Haute A (1983) Denitrification with methanol: Fundamental study of the growth and denitrification capacity of Hyphomicrobium sp. Water Research 17 (10):1249-1255. doi:http://dx.doi.org/10.1016/0043-1354(83)90249-X

158. Lettinga G (1995) Anaerobic digestion and wastewater treatment systems. Antonie van Leeuwenhoek 67 (1):3-28. doi:10.1007/bf00872193

9. Claus G, Kutzner H (1985) Denitrification of nitrate and nitric acid with methanol as carbon source. Appl Microbiol Biotechnol 22 (5):378-381. doi:10.1007/bf00582424

10. Foglar L, Briški F (2003) Wastewater denitrification process—the influence of methanol and kinetic analysis. Process Biochemistry 39 (1):95-103. doi:http://dx.doi.org/10.1016/S0032-9592(02)00318-7

11. Li M, Duraiswamy K, Knobbe M (2012) Adsorption enhanced steam reforming of methanol for hydrogen generation in conjunction with fuel cell: Process design and reactor dynamics. Chemical Engineering Science 67 (1):26-33. doi:http://dx.doi.org/10.1016/j.ces.2011.07.024

12. Pérez-Hernández R, Gutiérrez-Martínez A, Espinosa-Pesqueira ME, Estanislao ML, Palacios J Effect of the bimetallic Ni/Cu loading on the ZrO2 support for H2 production in the autothermal steam reforming of methanol. Catalysis Today (0). doi:http://dx.doi.org/10.1016/j.cattod.2014.08.009

13. Yi N, Si R, Saltsburg H, Flytzani-Stephanopoulos M (2010) Steam reforming of methanol over ceria and gold-ceria nanoshapes. Applied Catalysis B: Environmental 95 (1–2):87-92. doi:http://dx.doi.org/10.1016/j.apcatb.2009.12.012

14. Chiarello GL, Aguirre MH, Selli E (2010) Hydrogen production by photocatalytic steam reforming of methanol on noble metal-modified TiO2. Journal of Catalysis 273 (2):182-190. doi:http://dx.doi.org/10.1016/j.jcat.2010.05.012

15. Sharma S, Pollet BG (2012) Support materials for PEMFC and DMFC electrocatalysts—A review.

Journal of Power Sources 208 (0):96-119. doi:http://dx.doi.org/10.1016/j.jpowsour.2012.02.011

16. Motokura K, Nishimura D, Mori K, Mizugaki T, Ebitani K, Kaneda K (2004) A Ruthenium-Grafted Hydrotalcite as a Multifunctional Catalyst for Direct α-Alkylation of Nitriles with Primary Alcohols. Journal of the American Chemical Society 126 (18):5662-5663. doi:10.1021/ja0491811

17. Arndtsen BA, Bergman RG, Mobley TA, Peterson TH (1995) Selective Intermolecular Carbon-Hydrogen Bond Activation by Synthetic Metal Complexes in Homogeneous Solution. Accounts of Chemical Research 28 (3):154-162. doi:10.1021/ar00051a009

18. Blum O, Stöckigt D, Schröder D, Schwarz H (1992) O□
H Bond Activation in the Gas Phase: The
Reactions of Water and Methanol with [FeCH3]+. Angewandte Chemie International Edition in English 31 (5):603-604. doi:10.1002/anie.199206031

19. Owen JS, Labinger JA, Bercaw JE (2006) Kinetics and Mechanism of Methane, Methanol, and Dimethyl Ether C−H Activation with Electrophilic Platinum Complexes. Journal of the American Chemical Society 128 (6):2005-2016. doi:10.1021/ja056387t

20. Deo G, Wachs IE (1994) Reactivity of Supported Vanadium Oxide Catalysts: The Partial Oxidation of Methanol. Journal of Catalysis 146 (2):323-334. doi:http://dx.doi.org/10.1006/jcat.1994.1071

21. Schager F, Seevogel K, Pörschke K-R, Kessler M, Krüger C (1996) Reversible Water and Methanol Activation at the PdSn Bond1. Journal of the American Chemical Society 118 (51):13075-13076. doi:10.1021/ja962610y

22. Blanksby SJ, Ellison GB (2003) Bond Dissociation Energies of Organic Molecules. Accounts of Chemical Research 36 (4):255-263. doi:10.1021/ar020230d

23. Sun X, Sun X, Geng C, Zhao H, Li J (2014) Benchmark Study on Methanol C–H and O–H Bond Activation by Bare [FeIVO]2+. The Journal of Physical Chemistry A 118 (34):7146-7158. doi:10.1021/jp505662x

24. Donald WA, McKenzie CJ, O'Hair RAJ (2011) C-H Bond Activation of Methanol and Ethanol by a High-Spin FeIVO Biomimetic Complex. Angewandte Chemie International Edition 50 (36):8379-8383. doi:10.1002/anie.201102146

1625. Zhang CJ, Hu P (2001) A first principles study of methanol decomposition on Pd(111): Mechanisms for O–H bond scission and C–O bond scission. The Journal of Chemical Physics 115 (15):7182-7186. doi:doi:http://dx.doi.org/10.1063/1.1405157

26. Lee WT, Thomas F, Masel RI (1998) Methanol oxidation on (2×1)Pt(110): does the C–O or O–H bond break first? Surface Science 418 (2):479-483. doi:http://dx.doi.org/10.1016/S0039-6028(98)00761-4

27. Wang D, Farquhar ER, Stubna A, Münck E, Que L (2009) A diiron(iv) complex that cleaves strong C–H and O–H bonds. Nat Chem 1 (2):145-150. doi:http://www.nature.com/nchem/journal/v1/n2/suppinfo/nchem.162_S1.html

28. Sánchez VnM, Cojulun JA, Scherlis DnA (2010) Dissociation Free Energy Profiles for Water and Methanol on TiO2 Surfaces. The Journal of Physical Chemistry C 114 (26):11522-11526. doi:10.1021/jp102361z

29. Desai SK, Neurock M, Kourtakis K (2002) A Periodic Density Functional Theory Study of the Dehydrogenation of Methanol over Pt(111). The Journal of Physical Chemistry B 106 (10):2559-2568. doi:10.1021/jp0132984

30. Gu X-K, Li W-X (2010) First-Principles Study on the Origin of the Different Selectivities for Methanol Steam Reforming on Cu(111) and Pd(111). The Journal of Physical Chemistry C 114 (49):21539-21547. doi:10.1021/jp107678d

31. Lin S, Ma J, Zhou L, Huang C, Xie D, Guo H (2013) Influence of Step Defects on Methanol Decomposition: Periodic Density Functional Studies on Pd(211) and Kinetic Monte Carlo Simulations. The Journal of Physical Chemistry C 117 (1):451-459. doi:10.1021/jp310600q

32. Mei D, Xu L, Henkelman G (2009) Potential Energy Surface of Methanol Decomposition on Cu(110). The Journal of Physical Chemistry C 113 (11):4522-4537. doi:10.1021/jp808211q

33. Wang H, He C-z, Huai L-y, Liu J-y (2013) Decomposition and Oxidation of Methanol on Ir(111): A First-Principles Study. The Journal of Physical Chemistry C 117 (9):4574-4584. doi:10.1021/jp311227f

34. Mehmood F, Greeley J, Curtiss LA (2009) Density Functional Studies of Methanol Decomposition on Subnanometer Pd Clusters. The Journal of Physical Chemistry C 113 (52):21789-21796. doi:10.1021/jp907772c

35. Mehmood F, Greeley J, Zapol P, Curtiss LA (2010) Comparative Density Functional Study of Methanol Decomposition on Cu4 and Co4 Clusters†. The Journal of Physical Chemistry B 114 (45):14458-14466. doi:10.1021/jp101594z

36. Xie Y, Dong F, Heinbuch S, Rocca JJ, Bernstein ER (2009) Investigation of the reactions of small neutral iron oxide clusters with methanol. The Journal of Chemical Physics 130 (11):-. doi:doi:http://dx.doi.org/10.1063/1.3086724

37. Reber AC, Roach PJ, Woodward WH, Khanna SN, Castleman AW (2012) Edge-Induced Active Sites Enhance the Reactivity of Large Aluminum Cluster Anions with Alcohols. The Journal of Physical Chemistry A 116 (30):8085-8091. doi:10.1021/jp3047196

38. Feyel S, Schröder D, Schwarz H (2009) Pronounced Cluster-Size Effects: Gas-Phase Reactivity of Bare Vanadium Cluster Cations Vn+ (n = 1−7) Toward Methanol. The Journal of Physical Chemistry A 113 (19):5625-5632. doi:10.1021/jp901565r

39. Tenney SA, Cagg BA, Levine MS, He W, Manandhar K, Chen DA (2012) Enhanced activity for supported Au clusters: Methanol oxidation on Au/TiO2(110). Surface Science 606 (15–16):1233-1243. doi:http://dx.doi.org/10.1016/j.susc.2012.04.002

40. Bobuatong K, Karanjit S, Fukuda R, Ehara M, Sakurai H (2012) Aerobic oxidation of methanol to formic acid on Au20-: a theoretical study on the reaction mechanism. Physical Chemistry Chemical Physics 14 (9):3103-3111. doi:10.1039/c2cp23446g

1741. Ichihashi M, Hanmura T, Yadav RT, Kondow T (2000) Adsorption and Reaction of Methanol Molecule on Nickel Cluster Ions, Nin+ (n = 3−11). The Journal of Physical Chemistry A 104 (51):11885-11890. doi:10.1021/jp0028610

42. Tenney SA, Shah SI, Yan H, Cagg BA, Levine MS, Rahman TS, Chen DA (2013) Methanol Reaction on Pt–Au Clusters on TiO2(110): Methoxy-Induced Diffusion of Pt. The Journal of Physical Chemistry C 117 (51):26998-27006. doi:10.1021/jp409618j

43. Zhao S, Tang H, Ren Y, Xu A, Wang J (2014) Density functional study of CH3OH binding on small cationic CunAum+ (n+m<5) clusters. Computational and Theoretical Chemistry 1037 (0):14-21. doi:http://dx.doi.org/10.1016/j.comptc.2014.03.020

44. Oh SH, Carpenter JE (1986) Platinum-rhodium synergism in three-way automotive catalysts. Journal of Catalysis 98 (1):178-190. doi:http://dx.doi.org/10.1016/0021-9517(86)90307-6

45. Bouriazos A, Mouratidis K, Psaroudakis N, Papadogianakis G (2008) Catalytic Conversions in Aqueous Media. Part 2. A Novel and Highly Efficient Biphasic Hydrogenation of Renewable Methyl Esters of Linseed and Sunflower Oils to High Quality Biodiesel Employing Rh/TPPTS Complexes. Catal Lett 121 (1-2):158-164. doi:10.1007/s10562-007-9314-3

46. Engler B, Koberstein* E, Schubert P (1989) Automotive exhaust gas catalysts: Surface structure and activity. Applied Catalysis 48 (1):71-92. doi:http://dx.doi.org/10.1016/S0166-9834(00)80267-5

47. Piscina PRdl, Homs N (2008) Use of biofuels to produce hydrogen (reformation processes). Chemical Society Reviews 37 (11):2459-2467. doi:10.1039/b712181b

48. Cao D, Wieckowski A, Inukai J, Alonso-Vante N (2006) Oxygen Reduction Reaction on Ruthenium and Rhodium Nanoparticles Modified with Selenium and Sulfur. Journal of The Electrochemical Society 153 (5):A869-A874. doi:10.1149/1.2180709

49. Vayssilov GN, Petrova GP, Shor EAI, Nasluzov VA, Shor AM, Petkov PS, Rosch N (2012) Reverse hydrogen spillover on and hydrogenation of supported metal clusters: insights from computational model studies. Physical Chemistry Chemical Physics 14 (17):5879-5890. doi:10.1039/c2cp23648f

50. Ivanova Shor EA, Nasluzov VA, Shor AM, Vayssilov GN, Rösch N (2007) Reverse Hydrogen Spillover onto Zeolite-Supported Metal Clusters: An Embedded Cluster Density Functional Study of Models M6 (M = Rh, Ir, or Au). The Journal of Physical Chemistry C 111 (33):12340-12351. doi:10.1021/jp0711287

51. Argo AM, Gates BC (2003) MgO-Supported Rh6 and Ir6: Structural Characterization during the Catalysis of Ethene Hydrogenation. The Journal of Physical Chemistry B 107 (23):5519-5528. doi:10.1021/jp026717l

52. Shetty S, van Santen RA, Stevens PA, Raman S (2010) Molecular steps for the syngas conversion on the Rh6 cluster. Journal of Molecular Catalysis A: Chemical 330 (1–2):73-87. doi:http://dx.doi.org/10.1016/j.molcata.2010.07.004

53. Kiran V, Ravikumar T, Kalyanasundaram NT, Krishnamurty S, Shukla AK, Sampath S (2010) Electro-Oxidation of Borohydride on Rhodium, Iridium, and Rhodium–Iridium Bimetallic Nanoparticles with

Implications to Direct Borohydride Fuel Cells. Journal of The Electrochemical Society 157 (8):B1201-B1208. doi:10.1149/1.3442372

54. Serna P, Yardimci D, Kistler JD, Gates BC (2014) Formation of supported rhodium clusters from mononuclear rhodium complexes controlled by the support and ligands on rhodium. Physical Chemistry Chemical Physics 16 (3):1262-1270. doi:10.1039/c3cp53057d

55. Hamilton SM, Hopkins WS, Harding DJ, Walsh TR, Haertelt M, Kerpal C, Gruene P, Meijer G, Fielicke A, Mackenzie SR (2011) Infrared-Induced Reactivity of N2O on Small Gas-Phase Rhodium Clusters. The Journal of Physical Chemistry A 115 (12):2489-2497. doi:10.1021/jp201171p

56. Torres MB, Aguilera-Granja F, Balbás LC, Vega A (2011) Ab Initio Study of the Adsorption of NO on the Rh6+ Cluster. The Journal of Physical Chemistry A 115 (30):8350-8360. doi:10.1021/jp202511w

1857. Barreteau C, Spanjaard D, Desjonquères MC (1998) Electronic structure and total energy of transition metals from an spd tight-binding method: Application to surfaces and clusters of Rh. Physical Review B 58 (15):9721-9731

58. Jinlong Y, Toigo F, Kelin W (1994) Structural, electronic, and magnetic properties of small rhodium clusters. Physical Review B 50 (11):7915-7924

59. Reddy BV, Nayak SK, Khanna SN, Rao BK, Jena P (1999) Electronic structure and magnetism of Rhn (n=2-13) clusters. Physical Review B 59 (7):5214-5222

60. Zhi-Qiang L, Jing-Zhi Y, Ohno K, Kawazoe Y (1995) Calculations on the magnetic properties of rhodium clusters. Journal of Physics: Condensed Matter 7 (1):47

61. Volkan Ortalan1 AU, Bruce C. Gates, Nigel D. Browning (2010) Towards full-structure determination of bimetallic nanoparticles with an aberration-corrected electron microscope. Nat Nano 5 (12):843-847

62. Bergamaski K, Gonzalez ER, Nart FC (2008) Ethanol oxidation on carbon supported platinum-rhodium bimetallic catalysts. Electrochimica Acta 53 (13):4396-4406. doi:http://dx.doi.org/10.1016/j.electacta.2008.01.060

63. de Souza JPI, Queiroz SL, Bergamaski K, Gonzalez ER, Nart FC (2002) Electro-Oxidation of Ethanol on Pt, Rh, and PtRh Electrodes. A Study Using DEMS and in-Situ FTIR Techniques. The Journal of Physical Chemistry B 106 (38):9825-9830. doi:10.1021/jp014645c

64. Shubina TE, Koper MTM (2002) Quantum-chemical calculations of CO and OH interacting with bimetallic surfaces. Electrochimica Acta 47 (22–23):3621-3628. doi:http://dx.doi.org/10.1016/S0013-4686(02)00332-8

65. McNicol BD, Rand DAJ, Williams KR (1999) Direct methanol–air fuel cells for road transportation. Journal of Power Sources 83 (1–2):15-31. doi:http://dx.doi.org/10.1016/S0378-7753(99)00244-X

66. Sen Gupta S, Datta J (2006) A comparative study on ethanol oxidation behavior at Pt and PtRh electrodeposits. Journal of Electroanalytical Chemistry 594 (1):65-72. doi:http://dx.doi.org/10.1016/j.jelechem.2006.05.022

67. Tao F, Grass ME, Zhang Y, Butcher DR, Aksoy F, Aloni S, Altoe V, Alayoglu S, Renzas JR, Tsung C-K, Zhu Z, Liu Z, Salmeron M, Somorjai GA (2010) Evolution of Structure and Chemistry of Bimetallic Nanoparticle Catalysts under Reaction Conditions. Journal of the American Chemical Society 132 (25):8697-8703. doi:10.1021/ja101502t

68. Tzi-Yi Wu Z-YK, Jiin-Jiang Jow,Chung-Wen Kuo,Cheng-Jang Tsai,Pin-Rong Chen,Ho-Rei Chen (2012) Co-electrodeposition of Platinum and Rhodium in Poly(3,4-ethylenedioxythiophene)-Poly(styrene sulfonic acid) as Electrocatalyst for Methanol Oxidation. International Journal of Electrochemical Science 7 (9):8076-8090

69. Li M, Zhou WP, Marinkovic NS, Sasaki K, Adzic RR (2013) The role of rhodium and tin oxide in the platinum-based electrocatalysts for ethanol oxidation to CO2. Electrochimica Acta 104 (0):454-461. doi:http://dx.doi.org/10.1016/j.electacta.2012.10.046

70. Hahn F, Beden B, Lamy C (1986) In situ infrared reflectance spectroscopic study of the adsorption of formic acid at a rhodium electrode. Journal of Electroanalytical Chemistry and Interfacial Electrochemistry 204 (1–2):315-327. doi:http://dx.doi.org/10.1016/0022-0728(86)80529-0

71. Watanabe M, Motoo S (1975) Electrocatalysis by ad-atoms: Part II. Enhancement of the oxidation of methanol on platinum by ruthenium ad-atoms. Journal of Electroanalytical Chemistry and Interfacial Electrochemistry 60 (3):267-273. doi:http://dx.doi.org/10.1016/S0022-0728(75)80261-0

72. Guo JW, Zhao TS, Prabhuram J, Chen R, Wong CW (2005) Preparation and characterization of a PtRu/C nanocatalyst for direct methanol fuel cells. Electrochimica Acta 51 (4):754-763.

doi:http://dx.doi.org/10.1016/j.electacta.2005.05.056

1973. Löffler MS, Natter H, Hempelmann R, Wippermann K (2003) Preparation and characterisation of Pt–Ru model electrodes for the direct methanol fuel cell. Electrochimica Acta 48 (20–22):3047-3051. doi:http://dx.doi.org/10.1016/S0013-4686(03)00375-X

74. Friedrich KA, Geyzers KP, Linke U, Stimming U, Stumper J (1996) CO adsorption and oxidation on a Pt(111) electrode modified by ruthenium deposition: an IR spectroscopic study. Journal of Electroanalytical Chemistry 402 (1–2):123-128. doi:http://dx.doi.org/10.1016/0022-0728(95)04237-7

75. Toshima N, Wang Y (1994) Preparation and Catalysis of Novel Colloidal Dispersions of Copper/Noble Metal Bimetallic Clusters. Langmuir 10 (12):4574-4580. doi:10.1021/la00024a031

76. Liu X, Tian D, Meng C (2012) DFT study on stability and structure of bimetallic AumPdn (N=38, 55, 79, N=m+n, m/n≈2:1 and 5:1) clusters. Computational and Theoretical Chemistry 999 (0):246-250. doi:http://dx.doi.org/10.1016/j.comptc.2012.09.012

77. Sahiner N, Ozay O, Aktas N, Inger E, He J (2011) The on demand generation of hydrogen from Co-Ni bimetallic nano catalyst prepared by dual use of hydrogel: As template and as reactor. International Journal of Hydrogen Energy 36 (23):15250-15258. doi:http://dx.doi.org/10.1016/j.ijhydene.2011.08.082

78. Wu Q, Eriksen WL, Duchstein LDL, Christensen JM, Damsgaard CD, Wagner JB, Temel B, Grunwaldt J-D, Jensen AD (2014) Influence of preparation method on supported Cu-Ni alloys and their catalytic properties in high pressure CO hydrogenation. Catalysis Science & Technology 4 (2):378-386. doi:10.1039/c3cy00546a

79. Rösch N, Petrova G, Petkov P, Genest A, Krüger S, Aleksandrov H, Vayssilov G (2011) Impurity Atoms on Small Transition Metal Clusters. Insights from Density Functional Model Studies. Topics in Catalysis 54 (5-7):363-377. doi:10.1007/s11244-011-9667-0

80. Mainardi DS, Balbuena PB (2003) Hydrogen and Oxygen Adsorption on Rhn (n = 1−6) Clusters. The Journal of Physical Chemistry A 107 (48):10370-10380. doi:10.1021/jp036093z

81. Frisch MJT, G. W.;Schlegel, H. B.;Scuseria, G. E.;, Robb MAC, J. R.; Scalmani, G.; Barone, V.; Mennucci,, B.; Petersson GAN, H.; Caricato, M.; Li, X.; Hratchian, H., P.; Izmaylov AFB, J.; Zheng, G.; Sonnenberg, J. L.; Hada, M.;, Ehara MT, K.; Fukuda, R.; Hasegawa, J.; Ishida, M.; Nakajima,, T.; Honda YK,

O.; Nakai, H.; Vreven, T.; Montgomery, J. A., Jr.;, Peralta PEO, F.; Bearpark, M.; Heyd, J. J.; Brothers, E.;, Kudin KNS, V. N.; Kobayashi, R.; Normand, J.;, Raghavachari KR, A.; Burant, J. C.; Iyengar, S. S.; Tomasi,, J.; Cossi MR, N.; Millam, N. J.; Klene, M.; Knox, J. E.; Cross, J., B.; Bakken VA, C.; Jaramillo, J.; Gomperts, R.; Stratmann, R., E.; Yazyev OA, A. J.; Cammi, R.; Pomelli, C.; Ochterski, J. W.;, Martin RLM, K.; Zakrzewski, V. G.; Voth, G. A.; Salvador,, P.; Dannenberg JJD, S.; Daniels, A. D.; Farkas, Ö.; Ortiz, J., V.; Cioslowski JF, D. J. (2009) Gaussian 09, Revision A.1. Gaussian, Inc, Wallingford CT

82. Srivastava AK, Misra N (2014) Structures, stabilities, electronic and magnetic properties of small RhxMny (x+y = 2–4) clusters. Computational and Theoretical Chemistry 1047 (0):1-5. doi:http://dx.doi.org/10.1016/j.comptc.2014.08.008

83. Harding DJ, Mackenzie SR, Walsh TR (2009) Density functional theory calculations of vibrational spectra of rhodium oxide clusters. Chemical Physics Letters 469 (1–3):31-34. doi:http://dx.doi.org/10.1016/j.cplett.2008.12.053

84. Da Silva JLF, Piotrowski MJ, Aguilera-Granja F (2012) Hybrid density functional study of small Rhn (n= 2- 15) clusters. Physical Review B 86 (12):125430

85. Camacho-Mendoza R, Aquino-Torres E, Cruz-Borbolla J, Alvarado-Rodríguez J, Olvera-Neria O, Narayanan J, Pandiyan T (2014) DFT analysis: Fe4 cluster and Fe(110) surface interaction studies with pyrrole, furan, thiophene, and selenophene molecules. Struct Chem 25 (1):115-126. doi:10.1007/s11224-013-0254-9

2086. Wang H-Q, Li H-F (2014) A combined stochastic search and density functional theory study on the neutral and charged silicon-based clusters MSi6 (M = La, Ce, Yb and Lu). RSC Advances 4 (56):29782-29793. doi:10.1039/c4ra03788j

87. Chan B, Yim W-L (2013) Accurate Computation of Cohesive Energies for Small to Medium-Sized Gold Clusters. Journal of Chemical Theory and Computation 9 (4):1964-1970. doi:10.1021/ct400047y

88. Yumura T, Nanba T, Torigoe H, Kuroda Y, Kobayashi H (2011) Behavior of Ag3 Clusters Inside a Nanometer-Sized Space of ZSM-5 Zeolite. Inorganic Chemistry 50 (14):6533-6542. doi:10.1021/ic2001514

89. Yang H-W, Lu W-C, Zhao L-Z, Qin W, Yang W-H, Xue X-Y (2013) Structures and Electronic Properties

of the SiAun (n = 17–20) Clusters. The Journal of Physical Chemistry A 117 (13):2672-2677. doi:10.1021/jp3004807

90. Ochterski JW (2000) Thermochemistry in gaussian. Gaussian Inc, Pittsburgh, PA:1-17

91. McQuarrie DA, Simon JD (1999) Molecular thermodynamics. University Science Books Sausalito, CA,

92. Geudtner G, Calaminici P, Carmona-Espíndola J, del Campo JM, Domínguez-Soria VD, Moreno RF, Gamboa GU, Goursot A, Köster AM, Reveles JU, Mineva T, Vásquez-Pérez JM, Vela A, Zúñinga-Gutierrez B, Salahub DR (2012) deMon2k. Wiley Interdisciplinary Reviews: Computational Molecular Science 2 (4):548-555. doi:10.1002/wcms.98

93. Aguilera-Granja F, Balbás LC, Vega A (2009) Study of the Structural and Electronic Properties of RhN and RuN Clusters (N < 20) within the Density Functional Theory. The Journal of Physical Chemistry A 113 (48):13483-13491. doi:10.1021/jp905188t

94. Beltrán M, Buendía Zamudio F, Chauhan V, Sen P, Wang H, Ko Y, Bowen K (2013) Ab initio and anion photoelectron studies of Rhn (n = 1 − 9) clusters. Eur Phys J D 67 (3):1-8.doi:10.1140/epjd/e2013-30547-2

95. Chien C-H, Blaisten-Barojas E, Pederson MR (1998) Magnetic and electronic properties of rhodium clusters. Physical Review A 58 (3):2196-2202

96. Mehmood F, Rankin RB, Greeley J, Curtiss LA (2012) Trends in methanol decomposition on transition metal alloy clusters from scaling and Bronsted-Evans-Polanyi relationships. Physical Chemistry Chemical Physics 14 (24):8644-8652. doi:10.1039/c2cp00052k

97. Frelink T, Visscher W, van Veen JAR (1995) On the role of Ru and Sn as promotors of methanol electro-oxidation over Pt. Surface Science 335 (0):353-360. doi:http://dx.doi.org/10.1016/0039-6028(95)00412-2

Graphical Abstract